Since January 2020 Elsevier has created a COVID-19 resource centre with free information in English and Mandarin on the novel coronavirus COVID-19. The COVID-19 resource centre is hosted on Elsevier Connect, the company's public news and information website.

Antiviral Research 93 (2012) 118–125

Contents lists available at SciVerse ScienceDirect

Antiviral Research

journal homepage: www.elsevier.com/locate/antiviral

In vitro anti-hepatitis B and SARS virus activities of a titanium-substituted-heteropolytungstate

Yan-fei Qi [a,1], Hong Zhang [b,1], Juan Wang [a], Yanfang Jiang [b], Jinhua Li [a], Ye Yuan [a], Shiyao Zhang [a], Kun Xu [a], Yangguang Li [c], Juan Li [a,*], Junqi Niu [b,*], Enbo Wang [c]

[a] School of Public Health, Jilin University, Changchun, Jilin 130021, PR China
[b] Department of Infectious Diseases of the 1st Hospital, Jilin University, Changchun, Jilin 130021, PR China
[c] Institute of Polyoxometalate Chemistry, Northeast Normal University, Changchun, Jilin 130024, PR China

ARTICLE INFO

Article history:
Received 2 March 2011
Revised 1 October 2011
Accepted 7 November 2011
Available online 23 November 2011

Keywords:
Heteropolytungstate
Antiviral activity
Hepatitis B virus
SARS virus
In vitro

ABSTRACT

A structural determined heteropolytungstate, $[K_4(H_2O)_8Cl][K_4(H_2O)_4PTi_2W_{10}O_{40}]\cdot NH_2OH$ **1**, has been synthesized and evaluated for *in vitro* antiviral activities against hepatitis B (HBV) and SARS virus. The identity and high purity of compound **1** were confirmed by elemental analysis, NMR, IR analysis and single-crystal X-ray diffraction. The compound **1**, evaluated in HepG 2.2.15 cells expressing permanently HBV, significantly reduced the levels of HBV antigens and HBV DNA in a dose-dependent and time-dependent manner. EC_{50} values were determined to be 54 μM for HBeAg, 61 μM for HBsAg and 2.66 μM for supernatant HBV DNA, as compared to 1671, 1570, 169 μM, respectively, for the commercially-available hepatitis B drug adefovir dipivoxil (ADV). Intracellular cccDNA, pgRNA and HBcAg were also found to be decreased by compound **1** in a concentration-dependent manner. Cytotoxicity results showed that compound **1** has low toxicity in HepG 2 cells with CC_{50} value of 515.20 μM. The results indicate that compound **1** can efficiently inhibit HBV replication in HepG 2.2.15 cells line *in vitro*. Additionally, compound **1** also shows high anti-SARS activity at an EC_{50} of 7.08 μM and toxicity with a CC_{50} of 118.6 μM against MDCK cells.

1. Introduction

Hepatitis B virus (HBV) infections continue to be a major public health problem worldwide (Barraud et al., 1999). More than 400 million people worldwide are currently infected with hepatitis B virus. Approximately 20% of HBV patients will develop chronic hepatitis, and are at significant risk of developing cirrhosis or liver hepatocarcinoma. HBV is the prototype of hepadnaviridae, a family of small enveloped hepatotropic DNA viruses that can infect the liver of human (Marion and Robinson, 1983). Chronic hepatitis B patients are commonly treated with either interferon alpha (INF-α), or the nucleoside analog lamivudine (3TC), adefovir, entecavir or telbivudine which are the synthetic reverse transcriptase inhibitors (De Clercq, 1999; Delmas et al., 2002; Buster and Janssen, 2006). However, none of these therapies are completely safe and effective. Although direct antiviral therapy with amivudine or adefovir could efficiently control chronic active hepatitis B, drug resistance or renal toxicity could develop progressively several months after the initiation of therapy. It is thus still urgently required to identify effective anti-HBV agents.

Polyoxometalates (POMs) are inorganic cluster-like complexes and constituted from oxide anion and transition metal cations. These complexes have shown potential applications in multitudinal fields such as catalysis, medicine and functional materials (Pope and Müller, 1991, 1994). Especially, the medicinal properties of POMs have been a subject of interest (Witvrouw et al., 2000; Judd et al., 2001; Shigeta et al., 2003; Yamase, 2005). These compounds have low toxicity for cultured cells, and relatively less expensive than the "chemical" antiviral drugs. Recently, POMs have been reported to inhibit the replication of RNA viruses and DNA viruses *in vitro* and *in vivo*, such as the human immunodeficiency virus, severe acute respiratory syndrome (SARS) virus, influenza virus and herpes simplex virus (Rhule et al., 1998; Dan et al., 2002). The activity of POMs against hepatitis B virus was also suggested by Zoulim (1999). The mechanism of action of POMs remains to be fully elucidated, but may occur at any of the life cycle stages, including viral adsorption, penetration, or reverse-transcription (Dan et al., 2002; Shigeta et al.,

Abbreviations: HBV, hepatitis B virus; INF-α, interferon alpha; 3TC, nucleoside analog lamivudine; POMs, Polyoxometalates; SARS, severe acute respiratory syndrome; DMEM, Dulbecco's Modified Eagle's Medium; FBS, fetal bovine serum; Vero-E_6, African green monkey kidney cells; MTT,3-(4,5-dimethylthiazol-2-yl)-2,5-diphenyl tetrazolium bromide; ADV, adefovir dipivoxil; CC_{50}, 50% cytotoxic dose; TI, therapeutic index; EC_{50}, 50% effective concentration; CC_0, maximal noncytotoxic concentration; EC_{90}, 90% effective concentration; MDCK, Madin–Darby canine kidney.

* Corresponding authors. Tel.: +86 431 85619419; fax: +86 431 85645486.
E-mail addresses: li_juan@jlu.edu.cn (J. Li), junqiniu@yahoo.com.cn (J. Niu).
[1] These authors contributed equally to this study.

0166-3542/$ - see front matter © 2011 Elsevier B.V. All rights reserved.
doi:10.1016/j.antiviral.2011.11.003

2003). Among the various POMs, keggin-type heteropolyoxotungstates $[PW_{10}Ti_2O_{40}]^{7-}$ (Domaille and Knoth, 1983; Ozeki and Yamase, 1991) shows high antiviral activity. The interesting biological results of $[PW_{10}Ti_2O_{40}]^{7-}$ prompted us to explore the antiviral activity of compounds containing $[PW_{10}Ti_2O_{40}]^{7-}$ anions as potential anti-HBV agents.

It was also reported that the heteropolyoxotungstates $[PW_{10}Ti_2O_{40}]^{7-}$ have broad-spectrum anti-RNA virus activity (Dan and Yamase, 2006). Therefore, it is necessary to further explore the antiviral activity of compounds containing $[PW_{10}Ti_2O_{40}]^{7-}$. Severe acute respiratory syndrome (SARS), a disease seriously threatening human health caused by the single-stranded RNA coronavirus, spread in 29 countries in early 2003, presenting a worldwide public health concern (Fouchier et al., 2003; Drosten et al., 2003; Ksiazek et al., 2003). The research attention in exploitation of anti-SARS treatments has been mainly focused on vaccines, antiviral drugs, and their integration of traditional Chinese medicine and western therapy. However, no effective therapeutic drug is available to date (Stadler et al., 2003).

As a part of our ongoing antiviral drug discovery program, a number of POM analogs have been synthesized and evaluated for their potential antiviral activity (Li et al., 2004a,b). Herein, the POM analog $[K_4(H_2O)_8Cl][K_4(H_2O)_4PTi_2W_{10}O_{40}]\cdot NH_2OH$ **1** was prepared and structurally characterized. The antiviral activities against hepatitis B virus and SARS virus of **1** were investigated *in vitro*. The results indicate that compound **1** exhibits strong antiviral activities against the HBV and SARS viruses with low cytotoxicity, indicating that it is a potential medicinal candidate against HBV and SARS viruses.

2. Experimental

2.1. General procedures

All the chemicals were of analytic grade and used without further purification. Compound **1**, was freshly prepared and characterized. W and Ti in **1** were determined by a Leaman inductively coupled plasma (ICP) spectrometer. Infrared spectrum was recorded in the range 400–4000 cm^{-1} on an Alpha Centaurt FT/IR Spectrophotometer using KBr pellets. The ^{183}W NMR spectrum was obtained on a Bruker Am-500 spectrometer operated at 500 MHz with D_2O as the solvent. Quantitative RT-PCR was performed with ABI 7300 Sequence Detection System (Roche, Germany).

2.2. Synthesis of $[K_4(H_2O)_8Cl][K_4(H_2O)_4PTi_2W_{10}O_{40}]\cdot NH_2OH$ *1*

Synthesis of compound **1**: 5.94 g (2.0 mmol) $K_7PTi_2W_{10}O_{40}\cdot 5H_2O$ (Domaille et al., 1983) was added into 50 mL distilled water with stirring. To this solution, 1.03 g (15.0 mmol) $NH_2OH\cdot HCl$ and 1.04 g (2.8 mmol) $LaCl_3\cdot 7H_2O$ was added in sequence. The solution was heated to 70 °C for more than 2 h in a water bath, then filtered and kept slow evaporation in an undisturbed place at room temperature. Colorless crystals of compound **1** were isolated in 1 week with the yield of 60% based on $K_7PTi_2W_{10}O_{40}\cdot 5H_2O$. Elemental analysis (%) calcd for **1** ($H_{27}ClK_8NO_{53}PTi_2W_{10}$): P, 0.97; K, 9.73; Ti, 2.99; W, 57.45; Found: P, 1.10; K, 9.71; Ti, 2.89; W, 56.55%. IR (KBr pellet, cm^{-1}): 3427(s), 1621(s), 1081(m), 1064(m), 1050(w), 959(s), 885(m), 788(s), 593(w), 488(s). ^{183}W NMR (25 °C, D_2O, ppm): −78.53, −111.79, −124.51, −126.03, −137.54.

2.3. X-ray crystallography

The measurement for compound **1** was collected on a Rigaku R-AXIS RAPID IP diffractometer with Mo-Kα monochromated radiation (λ = 0.71073 Å) at 150 K. Empirical absorption correction was applied. The structure was solved by the direct method and refined by the Full-matrix least-squares on F^2 using the SHELXL-97 software (Sheldrick, 1997). All of the non-hydrogen atoms except the disordered atoms O(1), OW(2), OW(3) and Cl(1) were refined anisotropically. All the crystallographic parameters are tabulated in Table 1. Images were created with the DIAMOND program.

2.4. Cell culture and treatment

HepG 2.2.15 cells (provided by the Department of Infectious Diseases of the 1st Hospital, Jilin University, PR China) were cultured in Dulbecco's Modified Eagle's Medium (DMEM; Gibco) containing a 10% fetal bovine serum (FBS; Gibco), 100 U/mL penicillin, 100 U/mL streptomycin, and 200 μg/mL G418 (growth medium). During the experiments, the cells were grown in the media as described above without G418. The cell lines were incubated at 37 °C in 5% carbon dioxide atmosphere. Prior to exposures to drugs, the cell viability was verified to be >85% according to the standard trypan blue exclusion test.

HepG 2 (provided by the Department of Infectious Diseases of the 1st Hospital, Jilin University, PR China) were cultured in Dulbecco's Modified Eagle's Medium (DMEM; Gibco) containing a 10% fetal bovine serum (FBS; Gibco), 100 U/mL penicillin, and 100 U/mL streptomycin. The cell lines were incubated at 37 °C in 5% carbon dioxide atmosphere.

SARS virus (provided by Academy of Military Medical Sciences, Beijing, PR China) was propagated in African green monkey kidney cells (Vero-E_6). Vero cells were propagated in DMEM supplemented with 10% FBS, 2 mM L-glutamine, 50 U/mL penicillin, 50 μg/mL streptomycin and bicabouate. The cell lines were incubated at 37 °C in 5% carbon dioxide atmosphere.

Drugs were sterilized by filtration prior to use. Each agent was dissolved in DMEM to generate the appropriate doses for experimentation. Non-treated cells (DMEM alone) were used as negative controls.

2.5. Anti-HBV activity of compound *1*

2.5.1. Cytotoxicity analysis

The cytotoxicity of compound **1** was determined using 3-(4,5-dimethylthiazol-2-yl)-2,5-diphenyl tetrazolium bromide

Table 1
Crystal data and structure refinements for **1**.

Compound	**1**
Formula	$H_{27}ClK_8NO_{53}PTi_2W_{10}$
Fw	3202.75
T (K)	293(2)
Crystal system	Tetragonal
Space group	P4/mnc
a (Å)	14.200(2)
b (Å)	14.200(2)
c (Å)	12.418(3)
α (°)	90
β (°)	90
γ (°)	90
V (Å^3)	2503.8(7)
Z	2
ρcalcd (g cm^{-3})	4.248
μ (mm^{-1})	24.041
Rint	0.0562
Reflections collected	16,509
Independent reflections	1501
Goodness-of-fit on F^2	1.103
R_1[a] [$I > 2\sigma(I)$]	0.0456
wR_2[b] [$I > 2\sigma(I)$]	0.1235

[a] $R_1 = \sum||F_0| - |F_C||/\sum|F_0|$.
[b] $wR_2 = \sum[w(F_0^2 - F_C^2)^2]/\sum[w(F_0^2)^2]^{1/2}$.

(MTT) assay as previously described (Kodama et al., 1996). The optical absorbance was read on a plate reader (BIO-RAD Co.) at a wavelength of 490 nm. Briefly, HepG 2 cells were plated on 96-well plates at a density of 5.0×10^4 cells/mL. After a 24 h in period of incubation, the dilutions of **1**, and ADV at different doses were added. HepG 2 cells in the negative control group were treated with the same volume of medium. After a period of incubation, MTT solution (0.15 mL, 5 mg/mL in 0.01 M PBS) was added to each well. The cells were incubated for another 4 h at 37 °C, and then DMSO (0.15 mL) was added. The cytotoxicity was measured by the reduction of MTT observed in mitochondria at 24, 48, and 72 h after the initial treatment. The CC_{50} was defined as the concentration of drug that achieved 50% cytotoxicity against cultured cells, as calculated by the Bliss method (Han et al., 2008).

2.5.2. ELISA detection of HBsAg and HBeAg levels

Supernatants of cells treated with compound **1** or ADV and non-treated cells were collected. The semi-quantitative detection of HBsAg and HBeAg were estimated using ELISA assay kits (Shanghai Kehua Co., Ltd., China).

2.5.3. HBV DNA extraction and analysis by quantitative real-time (q)PCR

The supernatants of treated and non-treated cells were collected. The HBV DNA from the medium was extracted using HBV Real Quant PCR kit (QIAGEN kits, China). The ABI 7300 Sequence Detection System (Applied Biosystems) was used to quantify the purified DNA. PCR was performed under the following conditions: 37 °C for 5 min and 94 °C for 1 min, followed by 42 amplification cycles at 95 °C for 5 s and 60 °C for 30 s.

2.5.4. qPCR and RT-PCR of intracellular HBV pgRNA and cccDNA

HepG 2.2.15 cells were harvested by trypsin digestion and washed three times with phosphate buffered saline (PBS, pH 7.3). Cells were counted and used to evaluate the presence of HBV replicative intermediates: 1×10^6 cells for cccDNA, 3×10^6 cells for pgRNA.

Total RNA was isolated from cells using the TRIZOL reagent (Invitrogen). For RT-PCR analysis, RNA was reverse-transcribed at 42 °C for 90 min using a commercially available cDNA synthesis kit (Invitrogen). PCR was performed with gene specific primers for HBV and β-actin: HBV nt2429–2451 (forward), 5′-CTCAATCTCGGGAATCTCAATGT-3′; HBV nt2659–2636 (reverse), 5′-TGGATAAAACCTAGCAGGCATAAT-3′; β-actin nt2396–2415 (forward), 5′-ACGGCCAGGTCATCACCAT-3′, β-actin nt2438–2457 (reverse), 5′-AGGCTGGAAGAGTGCCTCAG-3′. qPCR was performed on the ABI 7300 Sequence Detection System using the SYBR Green kit (Invitrogen).

A standard curve was constructed by the simultaneous amplification of serial dilutions of the expression plasmid encoding HBV. Target cDNAs were normalized to the endogenous RNA levels of β-actin. Gene expression was determined using the relative quantification: ΔΔCT = [(CT Target − CT β-actin) Test] − [(CT Target − CT β-actin) Control], where CT was the fractional cycle number that reached a fixed threshold, CTest was the test of HBV in compound **1** and ADV exposed groups, and CControl was the reference control (RNA from non-treated cells). The fold increase was calculated using $2^{-\Delta\Delta CT}$ (Livak and Schmittgen, 2001).

Since HBV cccDNA is structurally similar to plasmid, intracellular cccDNA was extracted from cells by an alkali lysis procedure with a Qiagen Plasmid Mini Kit (CA) in order to remove most of cellular chromosomal DNA and non-supercoiled relaxed circular (rcDNA). Purified cccDNA was dissolved in 50 μL TE buffer (10 mM, pH 8.0), and 10 μL of the product was further treated with Plasmid-Safe™ ATP-Dependent DNase (PSAD; Epicentre Technologies, WI) to remove any remaining single-stranded virus DNA, rcDNA or cellular chromosomal DNA.

Intracellular cccDNA was quantified by selective fluorescent PCR with Taqman® MGB probe capable of amplifying and checking cccDNA more efficiently than rcDNA. The HBV primers were: nt1562–1579 (forward), 5′-TTCTCATCTGCCGGACCG-3′; nt1883–1864 (reverse), 5′-CACAGCTTGGAGGCTTGAAC-3′. The Taqman MG B probes were: nt1836–1855 (reverse), 5′ FAM-CCTAAT CATCTC TTGTTCAT-MGB 3′. qPCR was performed to detect intracellular cccDNA by using the RealQuant PCR kit (Invitrogen).

2.5.5. Western blot detection of HBcAg

Cell lysates were prepared by using RIPA (radio immunoprecipitation assay) lysis buffer supplemented with 1% (v/v) phenylmethanesulfonylfluoride (PMSF; Biyuntian Co., Ltd., China). Proteins were separated by electrophoresis on an 8% sodium dodecyl sulfate–polyacrylamide gel, transferred onto Immobilon-P membranes (Millipore), and analyzed by standard Western blot technique using anti-HBcAg antibodies (Santa Cruz Biotechnologies). β-Actin (Santa Cruz Biotechnologies) was used as the normalization control.

*2.6. Anti-SARS virus activity assay of compound **1***

The anti-SARS virus activity was estimated by MTT assay (Sigma). The optical absorbance was read on a plate reader (BIO-RAD Co.) at a wavelength of 570 nm for MTT. Vero-E_6 cell cultures (2×10^5 cells/mL) were prepared in a 96-well plate. After a 24 h period of incubation, SARS virus stock (0.1 mL per well) and different doses of compound **1** (0.1 mL per well) were added. In the control group, 0.1 mL medium was added. The plates were incubated at 37 °C in a humidified 5% CO_2 atmosphere for 2 days until maximum cytopathic effects were observed in the untreated, negative control cultures. The cytopathic effects were quantitated by the MTT assay. Briefly, 30 μL of MTT solution prepared in DMEM was added to each well and plates were incubated at 37 °C for 4 h. The MTT solution was removed without disturbing the cells and 60 μL of DMSO was added to each well to dissolve formazan crystals. After gently shaking the plates for 5 min, the absorbance from each well was measured at 540 nm. The percentages of protection were calculated as $[(A - B)/(C - B) \times 100]$, where A, B, and C stand for the absorbances of wells containing compound **1** and virus (A), virus (B) and cell (C) only, respectively.

2.7. Statistical analysis

Data were expressed as mean ± SD (standard deviation). All experiments were performed in triplicate. Statistical significance was evaluated by the one-way analysis of variance (ANOVA) and Student's *t*-test. Multiple comparisons were statistically analyzed using SAS software version 8.0 (significance was established at $P < 0.05$).

3. Results

3.1. Structure determination of compound 1

X-ray crystallography shows that compound **1** consists of a 3-D polyoxoanion framework $[K_4(H_2O)_4PTi_2W_{10}O_{40}]^{3-}$, one-dimensional (1-D) chainlike $[K_4(H_2O)_8Cl]^{3+}$ cations and the isolated hydroxylamine NH_2OH. In compound **1**, the polyoxoanion $[PTi_2W_{10}O_{40}]^{7-}$ exhibits a well-known Keggin structure (Fig. 1A). The central P atom is surrounded by a cube of eight oxygen atoms with each oxygen site half-occupied. The P–O distance is 1.51(2) Å. In the two crystallographically unique surrounding metal sites of the polyoxoanion, there exists a site occupancy disorder in the W2 center, that is, both Ti and W2 atom share the same site with 25% occupancy, respectively, forming the polyoxoanion $[PTi_2W_{10}O_{40}]^{7-}$.

The W(Ti)–O distances can be grouped into three sets: M–O_t (terminal) 1.614(18)–1.694(12) Å, M–O_c (central) 2.47(2)–2.51(2) Å, and M–O_b (bridge) 1.861(14)–1.936(12) Å. It is noteworthy that all the surface oxygen atoms of $[PTi_2W_{10}O_{40}]^{7-}$ except the μ_2-O_3 are coordinated with the K centers, exhibiting an unusual high coordination mode (Fig. 1A).

In asymmetric unit of compound **1**, the K1 center (see Fig. 1B) is octa-coordinated with four μ_2-O atoms of one polyoxoanion (O2 and O5), two terminal oxygen atoms of other two polyoxoanions (O6), and two coordination water molecules (OW1 and OW3A). The K–O distances range from 2.640(11) to 2.900(15) Å. Thus, the K1 centers can be regarded as a joint to connect all the polyoxoanions together. The K2 center (Fig. 1C) also exhibits the eight coordination environment with two terminal O atoms (O4) of two polyoxoanions, four coordination water molecules (OW2 and OW3) and two Cl anions. The K–O distances are in the range of 2.39(2)–2.71(3) Å, while the K–Cl distance is 2.80(4) Å. It is interesting that all coordination atoms are shared by two K2 centers. Based on this connection mode, the K centers form a 1-D chain via these double-bridging atoms (Fig. 2A). In the asymmetric unit of **1**, OW2, OW3 and Cl possess the 50%, 50% and 12.5% occupancies, respectively, thus, the 1-D chainlike cations can be described as $[K_4(H_2O)_8Cl]^{3+}$.On the basis of above connection mode, a novel 3-D polyoxoanion "host" framework is formed by the polyoxoanion $[PTi_2W_{10}O_{40}]^{7-}$ and the K1 centers with 1-D square tunnels along *c* axis (Fig. 2B). Furthermore, the 1-D chainlike counter-cations $[K_4(H_2O)_8Cl]^{3+}$ serve as the "guest", residing in the 1-D tunnels of the 3-D polyoxoanion "host". The isolated NH_2OH molecules are also filled in the interspace of the framework.

The solid state FTIR spectrum of the compound **1** showed the characteristic asymmetric stretching vibrational peaks at 788 (W–O_c–W), 593, 488, 885 (W–O_b–W), 959 (W–O_d), and splitting of the triply degenerate PO_4 stretching mode is observed at 1081, 1064, 1050 cm^{-1}. These peaks suggest that the polyoxometalic moiety $[PTi_2W_{10}O_{40}]^{7-}$ of the title complex still retain the basic framework of the Keggin structure. The bands in the range 2806–3073 cm^{-1} is assigned to the hydrogen bonding association N–H. The peaks at 1629 and 3424(s) cm^{-1} are assigned to the O–H of the water molecule.

3.2. Anti-HBV activity

3.2.1. Cytotoxic effects of compound *1* on HepG 2 cells

The growth of the HepG 2 cells in the presence of various concentrations of compound **1** was examined. The results of the cytotoxicity experiments are given in Fig. 3. The cytotoxicity of

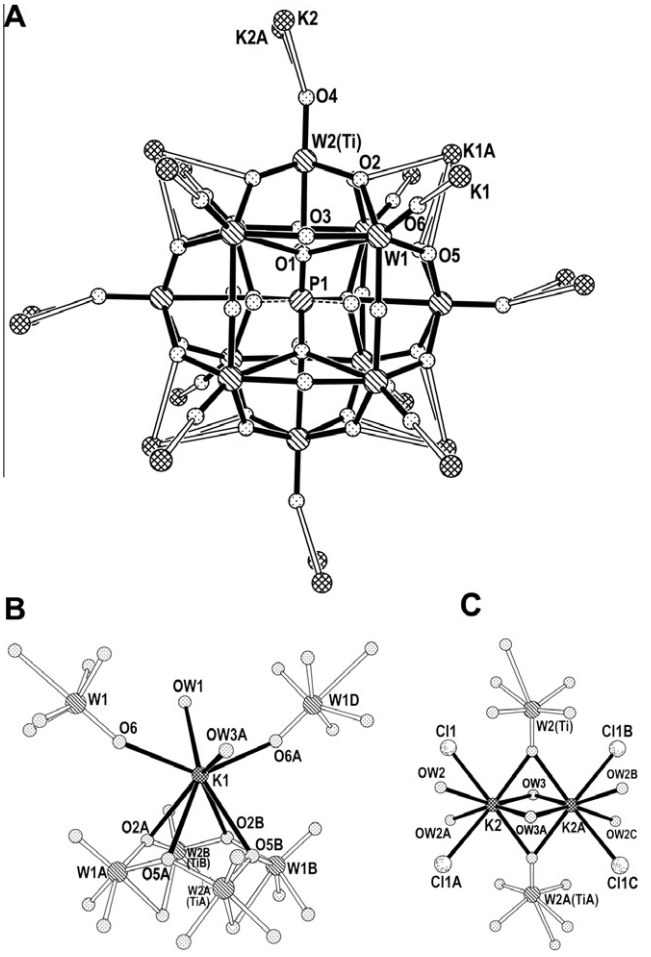

Fig. 1. (a) The structure of polyoxoanion of compound **1** showing the coordination sites with K centers. Coordination environments of (b) K1 center and (c) K2 center.

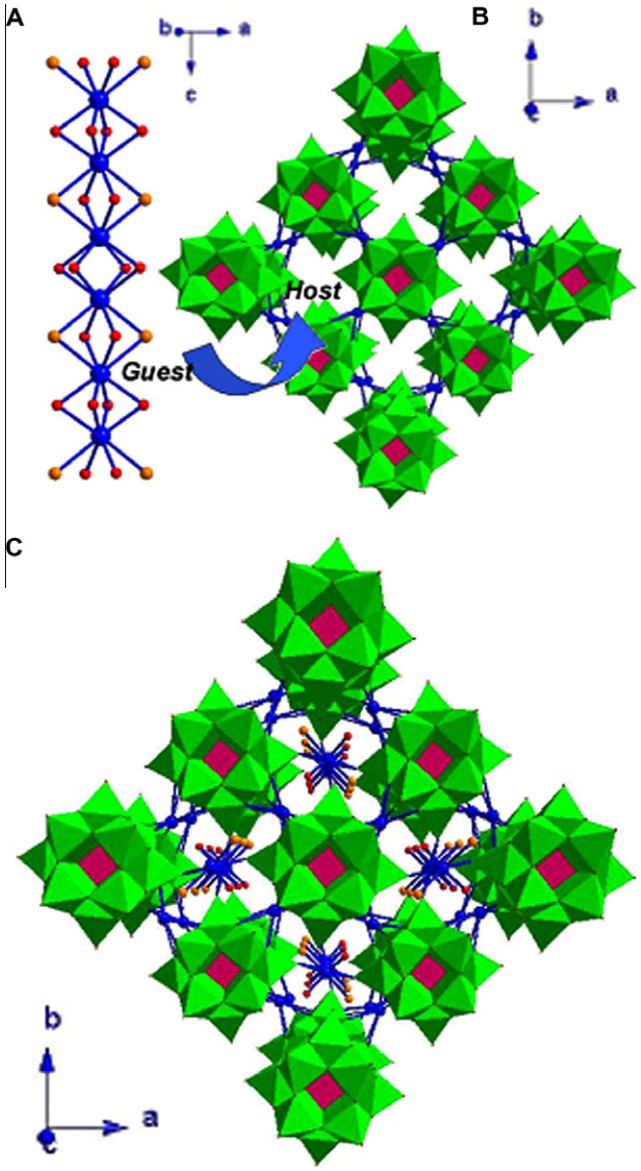

Fig. 2. View of compound **1**: the 1-D chainlike $[K_4(H_2O)_8Cl]^{3+}$ cation "guest" (A) are encapsulated in the 3-D porous $[K_4(H_2O)_4PTi_2W_{10}O_{40}]^{3-}$ polyoxoanion "host" (B) to from a novel "host–guest" compound **1** (C). The coordination water molecules OW(1) and OW(3) and the isolated NH_2OH molecules are omitted for clarity.

compound **1** on HepG 2 cells showed that the 50% cytotoxic dose (CC_{50}) of **1** and ADV was 515.20 and 1104.10 μM at 72 h, respectively. No obvious cytotoxicity was found for up to 72 h after treatment with compound **1** at lower concentrations (90 μM).

*3.2.2. Inhibitory effects of compound **1** on secreted HBeAg, HBsAg and HBV DNA expression in HepG 2.2.15 cultures*

The levels of HBsAg, HBeAg and extracellular HBV DNA in the medium were measured at different time points in the control group, ADV group, and compound **1** group, respectively, as shown in Fig. 4. After treatment, the levels of HBeAg, HBsAg and extracellular HBV DNA in the drug-treated groups were decreased significantly compared to that in the control group in a concentration-dependent manner ($P < 0.05$).

The levels of HBeAg, HBsAg and extracellular HBV DNA decreased with time in HepG 2.2.15 cells, indicating that the anti-HBV activity of compound **1** is time-dependent ($P < 0.01$). As shown in Fig. 4a, the inhibition ratio of HBeAg in compound **1**-treated cultures reached the peak value 65.89% at 93.38 μM at day 9 and still kept about 40.43% at day 11. At the same time, the inhibition ratio of HBsAg (shown in Fig. 4b) reached the peak value of 72.10% at 93.38 μM at day 9 and was still about 37.66% at day 11. The inhibition ratios of HBeAg and HBsAg in the ADV group were 57.03% and 56.22% at 2000 μM, respectively. The inhibitory values of HBeAg and HBsAg in ADV group decreased at day 11. Interestingly, the inhibition rates of compound **1** on extracellular HBV DNA at day 11 (4 days after the end of exposure to the drug) were lower than those observed on day 9. However, they were higher than those on day 7. At the same time, the inhibition values of ADV for extracellular HBV DNA declined and they were lower than the values at day 7, as shown in Fig. 4c. These result indicate that compound **1** may have a persistent effect on suppressing HBV.

The 50% effective concentration (EC_{50}) values of HBeAg, HBsAg and extracellular HBV DNA for compound **1** and ADV are shown in Table 2. The therapeutic index (TI) of compound **1** was higher than that of ADV.

*3.2.3. Inhibitory effects of compound **1** on intracellular cccDNA replication and pgRNA transcription in HepG 2.2.15 cells*

To characterize the anti-HBV mechanism of compound **1**, the amounts of intracellular viral pgRNA and DNA were measured in the control group, ADV group, and compound **1** group at different concentrations, respectively, at day 5, as shown in Fig. 5. The results revealed that the levels of intracellular HBV pgRNA and cccDNA were decreased with elevation of the compound **1** concentration, as compared to those detected from the control group ($P < 0.05$). The maximum inhibition ratios of pgRNA and DNA were 36.50% and 92.57% at 100 μM in the compound **1** group, which are higher than the ratios in the positive control group (AVD group, $P < 0.05$). These results suggested that compound **1** apparently impacting viral cccDNA replication and viral pgRNA transcription in HepG 2.2.15 cells, and that the anti-HBV mechanism of compound **1** seems to be similar to that of ADV.

*3.2.4. Inhibitory effects of compound **1** on intracellular HBcAg in HepG 2.2.15 cells*

The inhibitory effects of ADV and compound **1** on HBs(c)Ag protein levels were determined with Western blot. HepG 2.2.15 cells were treated with compound **1** and ADV, respectively. The cell extracts were prepared and analyzed at day 5. As shown in Fig. 6, the levels of intracellular protein levels of HBcAg were reduced with elevation of the compound **1** concentration in comparison with that in the control group ($P < 0.05$), indicating that the anti-HBV HBcAg activity of compound **1** is concentration-dependent. In addition, the inhibitory effect of compound **1** was higher than that of ADV at the same dose.

3.3. Anti-SARS virus activity

Aiming at evaluating the antiviral activity against SARS virus of compound **1**, the cytotoxicity of compound **1** in Vero-E_6 cells was first measured. The results showed that the maximal noncytotoxic concentration (CC_0) and the 50% cytotoxic concentration (CC_{50}) of compound **1** were 31.2 μM and 118.6 μM, respectively. According

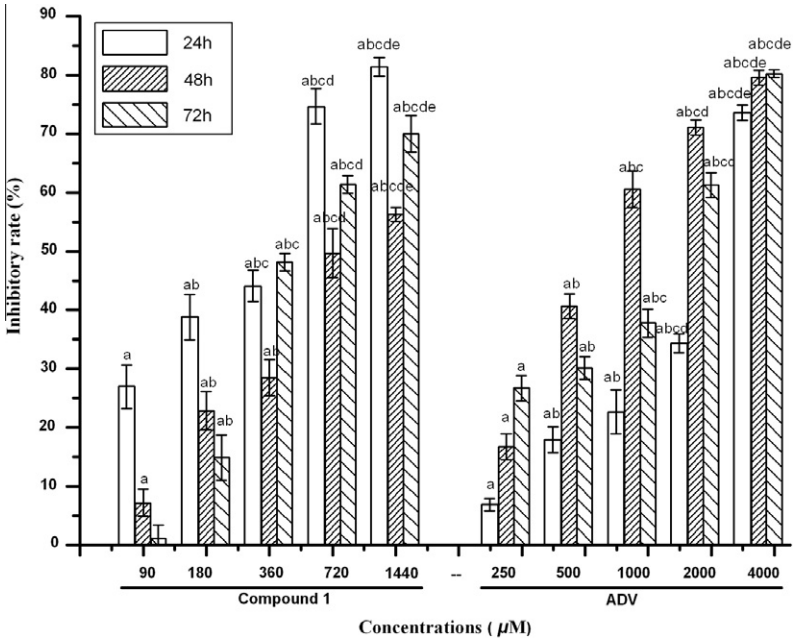

Fig. 3. Cytotoxicity of compound **1** and ADV in HepG 2 cells. [a]$P < 0.05$ for the drug groups vs. control group. For compound **1**: [b]$P < 0.05$ for the drug group vs. drug at 90 μM group. [c]$P < 0.05$ for the drug groups vs. drug at 180 μM group. [d]$P < 0.05$ for the drug group vs. drug at 360 μM group. [e]$P < 0.05$ vs. drug at 720 μM group. For ADV: [b]$P < 0.05$ for the drug group vs. drug at 250 μM group. [c]$P < 0.05$ for the drug groups vs. drug at 500 μM group. [d]$P < 0.05$ for the drug group vs. drug at 1000 μM group. [e]$P < 0.05$ vs. drug at 2000 μM group.

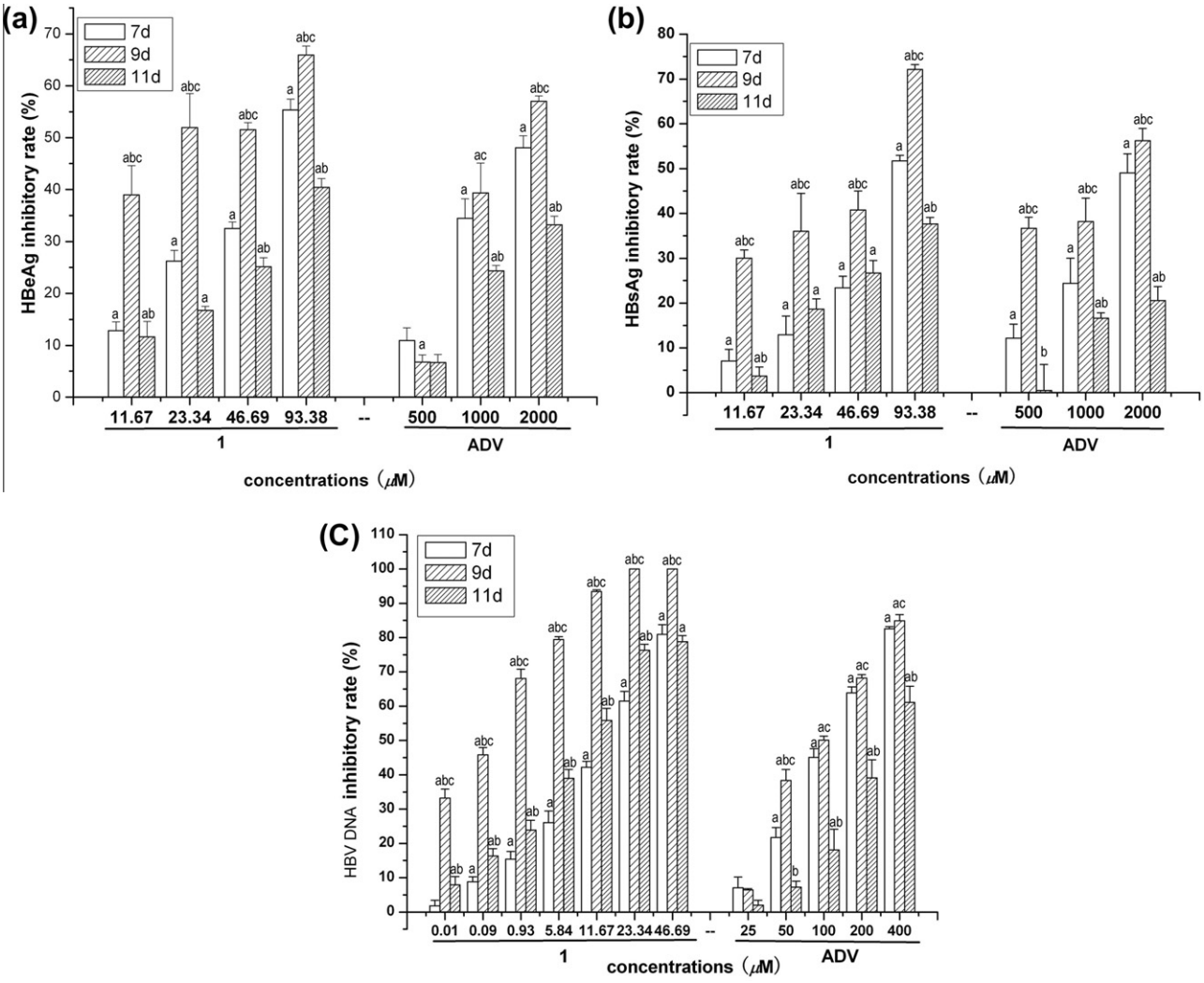

Fig. 4. The inhibitor effect of control group, ADV groups, and compound **1** groups on secretion of HBeAg (a), HBsAg (b) and extracellular viral DNA (c) from the medium of HepG 2.2.15 cells. [a] $P < 0.05$ vs. the corresponding negative control. [b] $P < 0.05$ vs. the corresponding 7 days outcome of the same dose. [c] $P < 0.05$ vs. the corresponding 11 days outcome of the same dose.

Table 2
Anti-HBV activity, cytotoxicity and the selective index (TI) of compound **1** and ADV *in vitro*.

	HBeAg		HBsAg		HBV DNA	
	1	ADV	1	ADV	1	ADV
EC_{50}[a] (μM)	54	1671	61	1570	2.66	169
CC_{50}[b] (μM)	515.20	1104.10	515.20	1104.10	515.20	1104.10
TI[c]	9.54	0.66	8.45	0.70	193.68	6.53

[a] The concentrations of **1** or ADV needed to inhibit HBV-DNA replication, or HBsAg and HBeAg secretions to 50% (EC_{50}).
[b] The cytotoxicity concentration of **1** or ADV that reduced cell viability to 50% (CC_{50}).
[c] $TI = CC_{50}/EC_{50}$.

to the cytotoxic results, compound **1** was diluted at five non-toxic concentrations (31.2, 15.6, 7.8, 3.9, and 1.95 μM) and the anti-SARS virus activity was checked with MTT assay. As shown in Fig. 7, the inhibition ratio of compound **1** increased with concentration, indicating that the anti-SARS virus activity of compound **1** is concentration-dependent. It is noteworthy that the SARS virus was completely inhibited at 31.2 μM. The 50% effective concentration (EC_{50}) and the 90% effective concentration (EC_{90}) were 7.08 and 21.0 μM, respectively. TI of compound **1** was 16.75.

4. Discussion

Currently, nucleoside analogs play an important role in the therapy of HBV, however, some disadvantages of these agents include side effects, drug resistance and costs which limit their clinical use in HBV-infected patients. Polyoxometalates, as non-nucleoside analogs, have been proven to exhibit broad inhibitory activity against human immunodeficiency viruses (HIV-1 and HIV-2), herpes simplex virus, and influenza virus. Especially, the titanium-containing polyoxotungstates have shown antiviral activity against a variety of enveloped RNA or DNA viruses. Herein, we synthesized a titanium-substituted-heteropolytungstate $[K_4(H_2O)_8Cl][K_4(H_2O)_4PTi_2W_{10}O_{40}]\cdot NH_2OH$, and examined the anti-HBV activities *in vitro*. HepG 2.2.15 cells as a useful "*in vitro*" model are widely used for the evaluation of novel anti-HBV drugs and chosen in our experiments. The cell line contains multiple copies of HBV genome that can stably integrate into the host cell genome. The results indicate that compound **1** inhibited HBV DNA, HBsAg and HBeAg antigens in the culture medium in a concentration-and-time dependent manner. A lower concentration of the compound **1** was required to effectively inhibit secreted HBV DNA than to inhibit secreted antigens. It is possible that the compound acts on the exported virions outer protein coats. Although the mechanisms mediating the antiviral effects by compound **1** remain un-

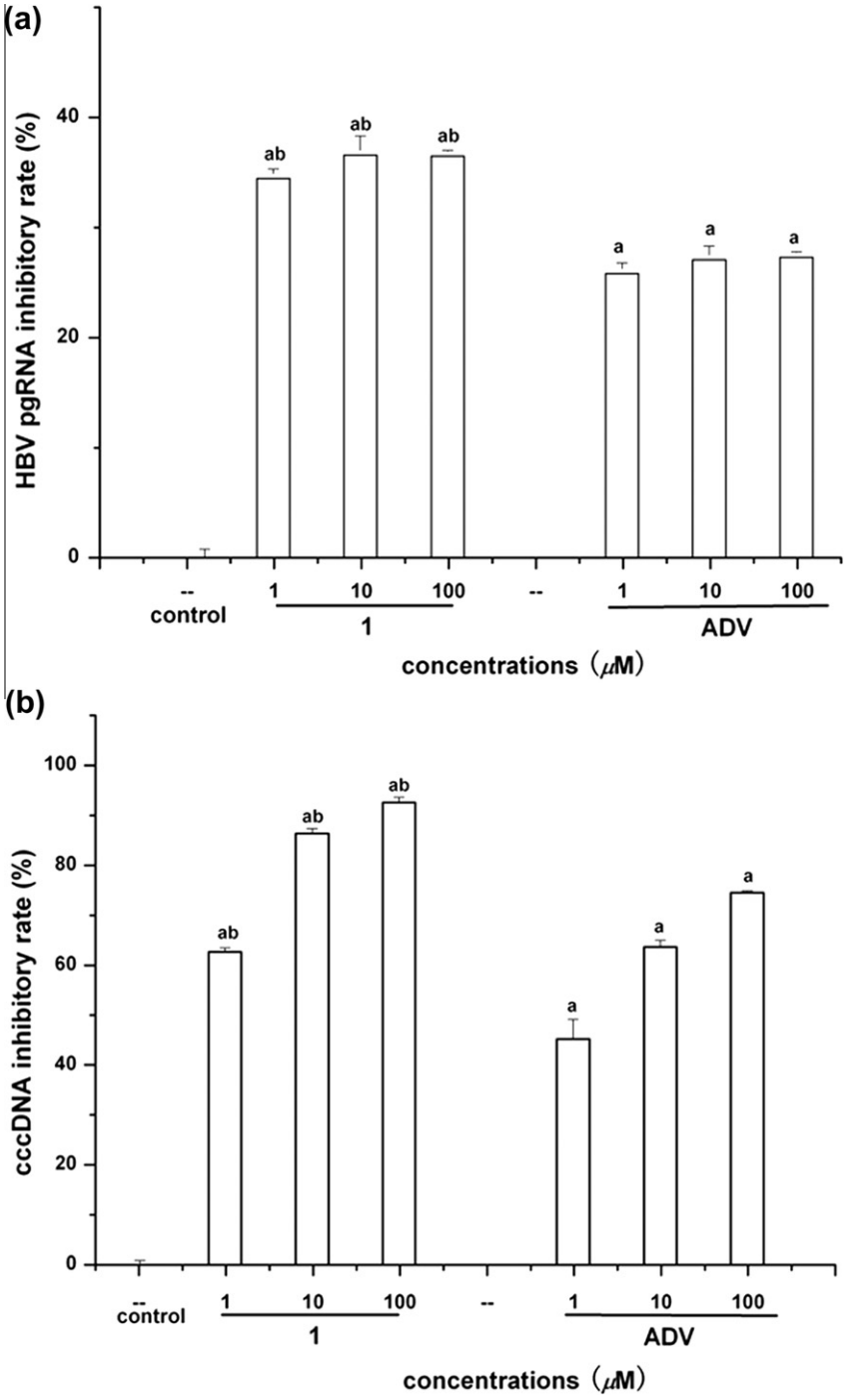

Fig. 5. The inhibition effect on the levels of intracellular pgRNA (a) and cccDNA (b) in control group, ADV groups, and compound **1** groups at different concentrations. [a]$P < 0.05$ vs. the corresponding negative control. [b]$P < 0.05$ vs. the corresponding ADV groups at the same concentration.

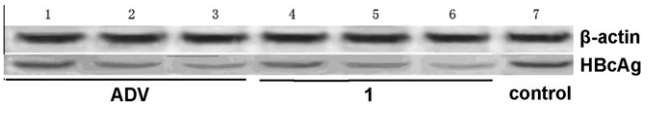

Fig. 6. Western blot analysis of the expression of HBcAg in HepG 2.2.15 cells. β-Actin was used as the internal reference. Lane 1: ADV (1 μM); lane 2: ADV (10 μM); lane 3: ADV (100 μM); lane 4: Compound **1** (1 μM); lane 5: Compound **1** (10 μM); lane 6: Compound **1** (100 μM); lane7: negative control.

clear, we have deduced that compound **1** might block the secretion of HBV containing nucleocapsids or destabilize HBV DNA-containing nucleocapsids. Interestingly, we observed that the *in vitro* anti-HBV properties of compound **1** against rebound of serum HBV DNA, HBsAg and HBeAg were more robust than those of positive group, ADV, as indicated by evaluation of treated cells 4 days after termination of treatment. This result shows that compound **1** has a sustained anti-HBV activity.

The levels of intracellular HBV DNA, RNA and HBcAg protein were also reduced by compound **1** in a concentration-dependent manner. The ADV drug competitively inhibits HBV polymerase, which is structurally similar to dATP. It is known to reduce the levels of HBV DNA and HBsAg both *in vitro* and *in vivo* by a phosphorylation event that facilitates its physical incorporation into nascent

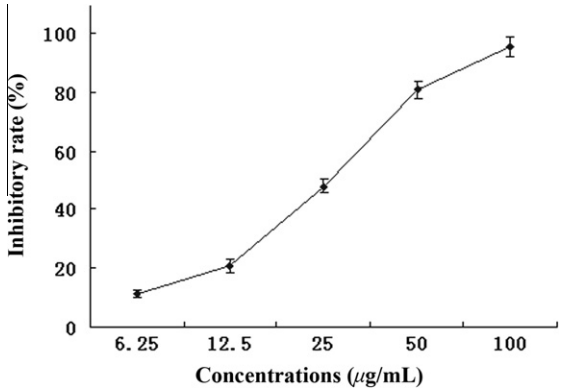

Fig. 7. The inhibition of **1** to SARS virus in different concentrations.

viral DNA by the activity of HBV polymerase during replication. In our study, we observed an apparent reduction in the levels of intracellular HBV-specific RNA and DNA following compound **1** treatment. These data also reveal that the anti-HBV mechanism of compound **1** may be similar to that of the nucleoside analog. Since the HBV pgRNAs were transcribed from cccDNA, we presume that HBV-specific transcripts may be affected by compound **1**. It is also important to consider that the HBV pgRNA was inhibited in drug-treated cells (He et al., 2008). HBcAg, HBsAg and HBV polymerase are translated from pregenome mRNA, and the minus strand HBV DNA are transcribed from the pregenome mRNA template. In this study, it was found that compound **1** could inhibit the levels of HBcAg, HBsAg and HBV DNA protein expressed in a concentration-dependent manner *in vitro*. These results suggested that compound **1** apparently interfered with viral pgRNA transcription in HepG 2.2.15 cells.

Moreover, compound **1** shows broad-spectrum antiviral activity. It can efficiently inhibit SARS virus in Vero-E_6 cells *in vitro* with low toxicity against MDCK cells. In summary, a heteropolytungstate has been prepared and characterized. The *in vitro* experimental results show that compound **1** has potential anti-HBV and anti-SARS virus activities. Further experiments are underway now, which include evaluation of *in vivo* activities and determination of the mechanism of anti-HBV activity of compound **1**.

Acknowledgements

This work was financially supported by the National S & T Major Project of China (2009ZX09103-105), Research Foundation of Jilin University (200904014, 200903115 and 20111070), SRFDP (2009 0061 120093), China Postdoctoral Science Foundation (20100481064) and S & T Development Project Foundation of Jilin Province (201101057).

Appendix A. Supplementary data

Supplementary data associated with this article can be found, in the online version, at doi:10.1016/j.antiviral.2011.11.003.

References

Barraud, L., Guerret, S., Chevallier, M., Borel, C., Jamard, C., Trépo, C., Wild, C.P., Cova, L., 1999. Enhanced duck hepatitis B virus gene expression following aflatoxin B1 exposure. Hepatology 29, 1317–1323.

Buster, E.H., Janssen, H.L., 2006. Antiviral treatment for chronic hepatitis B virus infection–immune modulation or viral suppression? Neth. J. Med. 64, 175–185.

Dan, K., Miyashita, K., Seto, Y., Fujita, H., Yamase, T., 2002. The memory effect of heteropolyoxotungstate (PM-19) pretreatment on infection by herpes simplex virus at the penetration stage. Pharmacol. Res. 46, 357–361.

Dan, K., Yamase, T., 2006. Prevention of the interaction between HVEM, herpes virus entry mediator, and gD, HSV envelope protein, by a Keggin polyoxotungstate, PM-19. Biomed. Pharmacother. 60, 169–173.

De Clercq, E., 1999. Perspectives for the treatment of hepatitis B virus infections. Int. J. Antimicrob. Agents 12, 81–95.

Delmas, J., Schorr, O., Jamard, C., Gibbs, C., Trépo, C., Hantz, O., Zoulim, F., 2002. Inhibitory effect of adefovir on viral DNA synthesis and covalently closed circular DNA formation in duck hepatitis B virus-infected hepatocytes in vivo and in vitro. Antimicrob. Agents Chemother. 46, 425–433.

Domaille, P.J., Knoth, W.H., 1983. $Ti_2W_{10}PO_{40}^{7-}$ and $[CpFe(CO)_2Sn]_2W_{10}PO_{38}^{5-}$. Preparation, properties, and structure determination by tungsten-183 NMR. Inorg. Chem. 22, 818–822.

Drosten, C., Günther, S., Preiser, W., van der Werf, S., Brodt, H., Becker, S., Rabenau, H., Panning, M., Kolesnikova, L., Fouchier, R.A.M., Berger, A., Burguière, A., Cinatl, J., Eickmann, M., Escriou, N., Grywna, K., Kramme, S., Manuguerra, J., Müller, S., Rickerts, V., Stürmer, M., Vieth, S., Klenk, H., Osterhaus, A.D.M.E., Schmitz, H., Doerr, H.W., 2003. Identification of a novel coronavirus in patients with severe acute respiratory syndrome. N. Engl. J. Med. 348, 1967–1976.

Fouchier, R.A.M., Kuiken, T., Schutten, M., van Amerongen, G., van Doornum, G.J.J., van den Hoogen, B.G., Peiris, M., Lim, W., Stohr, K., Osterhaus, A.D.M.E., 2003. Aetiology: Koch's postulates fulfilled for SARS virus. Nature 423, 240.

Han, Y.Q., Huang, Z.M., Yang, X.B., Liu, H.Z., Wu, G.X., 2008. In vivo and in vitro anti-hepatitis B virus activity of total phenolics from *Oenanthe javanica*. J. Ethnopharmacol. 118, 148–153.

He, Y.W., Guo, C.X., Pan, Y.F., Peng, C., Weng, Z.H., 2008. Inhibition of hepatitis B virus replication by pokeweed antiviral protein in vitro. World J. Gastroenterol. 14, 1592–1597.

Judd, D.A., Nettles, J.H., Nevins, N., Snyder, J.P., Liotta, D.C., Tang, J., Ermolieff, J., Schinazi, R.F., Hill, C.L., 2001. Polyoxometalate HIV-1 protease inhibitors. A new mode of protease inhibition. J. Am. Chem. Soc. 123, 886–897.

Kodama, E., Shigeta, S., Suzuki, T., De Clercq, E., 1996. Application of a gastric cancer cell line (MKN-28) for anti-adenovirus screening using the MTT method. Antiviral Res. 31, 159–164.

Ksiazek, T.G., Erdman, D., Goldsmith, C.S., Zaki, S.R., Peret, T., Emery, S., Tong, S., Urbani, C., Comer, J.A., Lim, W., Rollin, P.E., Dowell, S.F., Ling, A.E., Humphrey, C.D., Shieh, W.J., Guarner, J., Paddock, C.D., Rota, P., Fields, B., DeRisi, J., Yang, J.Y., Cox, N., Hughes, J.M., LeDuc, J.W., Bellini, W.J., Anderson, L.J., 2003. A novel coronavirus associated with severe acute respiratory syndrome. N. Engl. J. Med. 348, 1953–1966.

Li, J., Qi, Y.F., Li, J., Wang, H.F., Wu, X.Y., Duan, L.Y., Wang, E.B., 2004a. Heteropolymolybdate–amino acid complexes: synthesis, characterization and biological activity. J. Coord. Chem. 57, 1309–1319.

Li, J., Qi, Y.F., Wang, E.B., Li, J., Wang, H.F., Li, Y.G., Lu, Y., Hao, N., Xu, L., Hu, C.H., 2004b. Synthesis, structural characterization and biological activity of polyoxometalate-containing protonated amantadine as a cation. J. Coord. Chem. 57, 715–721.

Livak, K.J., Schmittgen, T.D., 2001. Analysis of relative gene expression data using real-time quantitative PCR and the $2^{-\Delta\Delta CT}$ method. Methods 25, 402–408.

Marion, P.L., Robinson, W.S., 1983. Hepadna viruses: hepatitis B and related viruses. Curr. Top. Microbiol. Immunol. 105, 99–121.

Ozeki, T., Yamase, T., 1991. Structure of a dititanodecatungstophosphate. Acta Crystallogr. Sect. C 47, 693–696.

Pope, M.T., Müller, A., 1991. Polyoxometalate chemistry: an old field with new dimensions in several disciplines. Angew. Chem. Int. Ed. Engl. 30, 34–48.

Pope, M.T., Müller, A., 1994. Polyoxometalates: From Platonic Solids to anti-retroviral Activity. Kluwer Academic Publishers, Dordrecht.

Rhule, J.T., Hill, C.L., Judd, D.A., Schinazi, R.F., 1998. Polyoxometalates in medicine. Chem. Rev. 98, 327–358.

Sheldrick, G.M., 1997. SHELXL97, Program for Crystal Structure Refinement. University of Göttingen, Göttingen, Germany.

Shigeta, S., Mori, S., Kodama, E., Kodama, J., Takahashi, K., Yamase, T., 2003. Broad spectrum anti-RNA virus activities of titanium and vanadium substituted polyoxotungstates. Antiviral Res. 58, 265–271.

Stadler, K.M.V., Masignani, V., Eickmann, M., Becker, S., Abrignani, S., Klenk, H.D., Rappuoli, R., 2003. SARS – beginning to understand a new virus. Nat. Rev. Microbiol. 1, 209–218.

Witvrouw, M., Weigold, H., Pannecouque, C., Schols, D., De Clercq, E., Holan, G., 2000. Potent anti-HIV (type 1 and type 2) activity of polyoxometalates: structure–activity relationship and mechanism of action. J. Med. Chem. 43, 778–783.

Yamase, T., 2005. Anti-tumor, -viral, and -bacterial activities of polyoxometalates for realizing an inorganic drug. J. Mater. Chem. 15, 4773–4782.

Zoulim, F., 1999. Therapy of chronic hepatitis B virus infection: inhibition of the viral polymerase and other antiviral strategies. Antiviral Res. 44, 1–30.